An analysis of the forming speed variation with relation to deep drawing depth of steel DP 600 sheets

Márcio Madi, Miguel Vaz Júnior, Ravilson Antônio Chemim Filho & Paulo Victor Prestes Marcondes

The International Journal of Advanced Manufacturing Technology

ISSN 0268-3768
Volume 99
Combined 9-12

Int J Adv Manuf Technol (2018)
99:2417-2424
DOI 10.1007/s00170-018-2635-0

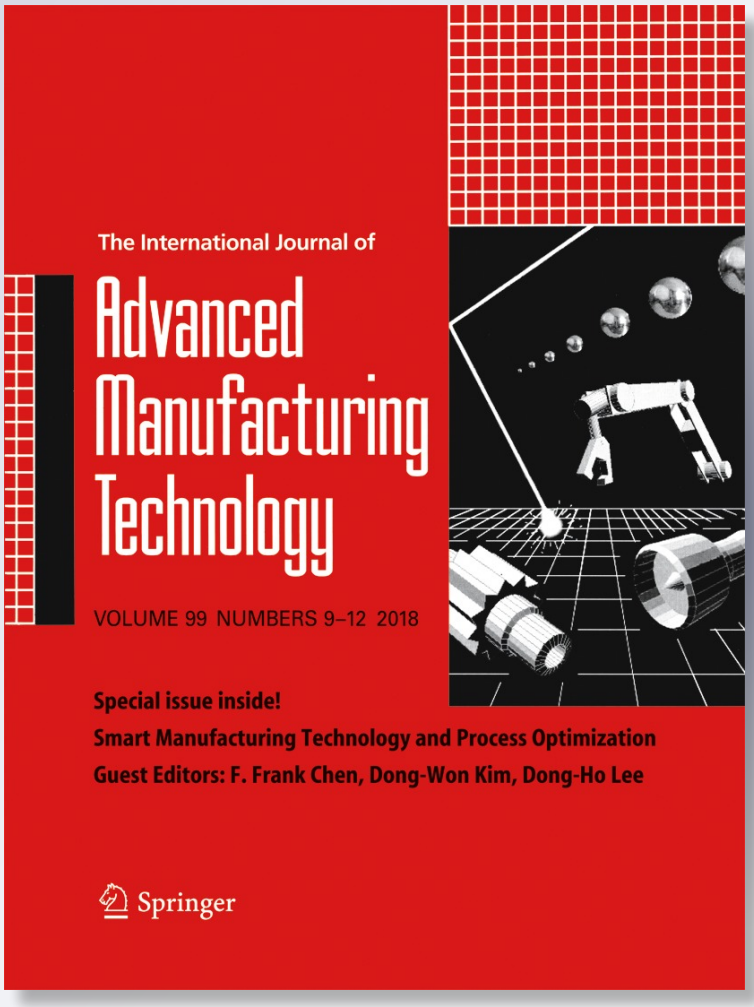

Springer

The International Journal of Advanced Manufacturing Technology (2018) 99:2417–2424
https://doi.org/10.1007/s00170-018-2635-0

ORIGINAL ARTICLE

An analysis of the forming speed variation with relation to deep drawing depth of steel DP 600 sheets

Márcio Madi[1] · Miguel Vaz Júnior[2] · Ravilson Antônio Chemim Filho[3] · Paulo Victor Prestes Marcondes[3]

Received: 2 May 2018 / Accepted: 21 August 2018 / Published online: 4 September 2018

Abstract
Stamping is a metal forming process which aims to manufacture shaped parts from flat sheets. The automotive industry has used this manufacturing process in large scale, thereby requiring development of numerical tools with objective of time and cost reduction. Use of ever thinner sheets has prompt study of forming mechanisms, in special ductile failure. This work is inserted within this framework, in which a numerical methodology to study ductile failure in stamping processes is proposed. Emphasis is placed on a strategy to determine an optimum forming speed based on assessment of failure onset. The technique was applied to a dual phase DP 600 steel. Strain paths in predefined directions were adopted to approach ductile failure onset and evolution. A forming limit curve determined experimentally in a previous work was used as failure criterion. The results indicate an optimum punch speed which allows maximum speed without failure onset.

Keywords DP 600 forming · Speed simulation · Failure criteria

1 Introduction and objectives

In recent decades, the increasing competition and demand for safer, cheaper, and less polluting cars have required investments from automotive manufacturers, steel companies, and the scientific community in searching for new types of steel. Such research effort led to significant increase in use of advanced high strength steels in vehicles.

The automotive industry has promoted huge advances in the metallurgical evolution of steels over the years. It suffices to remember that the first cars were basically square due to the inadequate stampability of ferritic-perlitic steel sheets; a consequence not only of the incipient metallurgical science of the time, but also of the limitations of the industrial processes of refining and forming. However, the pressure upon the automotive industry for reduction of prices and improvement in automobile design forced steel manufacturers to develop new technologies in order to produce high stampability steels.

The main objective of this sector has been to offer ever more innovative materials, as well as production and assembly techniques focused on obtaining an increasingly high level of confidence and an increasing reduction of vehicle weight, as discussed by Andrade et al. [1], De Cooman [2], and Grajcar [3].

At least three decades ago, the new steels—which emerged to meet the need for better formability—were classified within a single family, known as advanced high strength steels (AHSS). The increase of mechanical strength achieved with those steels almost inevitably led to reduction of its total elongation, that is, its stampability. However, the use of adequate microstructures allows minimizing the ductility loss.

The first specific development on dual phase (DP) steels appeared in the late 1970s [4]. One of the resources available to simultaneously maximize ductility and mechanical strength of steels consists of the use of microstructures more complex than ferritic or ferritic-perlitic microstructures, which are usually present in common low-carbon alloys.

In the study of fracture mechanisms in metallic materials, a good tool that has been used to establish the forming limit of the material—determined in laboratory scale—is the forming

✉ Márcio Madi
marcio.madi@ifpr.edu.br

Miguel Vaz Júnior
Miguel.vaz@udesc.br

Ravilson Antônio Chemim Filho
ravilson@ufpr.br

Paulo Victor Prestes Marcondes
marcondes@ufpr.br

[1] IFPR - Paraná Federal Institute of Education, Science and Technology, Curitiba, Brazil

[2] UDESC - State University of Santa Catarina, Curitiba, Brazil

[3] UFPR - Federal University of Paraná, Curitiba, Brazil

limit diagram (FLD). Such relation makes possible to conclude whether the material and process are adequate to manufacture an individual component. The FLD is an important tool to develop the application of a given product [5]. This concept, based on experimental measurements, was first introduced by Keeler [6] for the positive values of the minimum principal strain in the sheet plane, which was later extended by Goodwin [7] and Woodthorpe et al. [8] to the strain domain between uniaxial traction and biaxial stretching states.

In order to describe the plastic strain mechanism in steels and predict failure onset in those materials, models have been studied since the 1960s. However, there is no single model that can be considered for all forming processes and any materials. The existing models can be applied to specific characteristics or properties such as decrease of strength, void nucleation, and evolution of discontinuities.

Mechanical defects in a finished product indicate that the choice of forming parameters was not proper. The individual and interactive effects of forming depth, direction and speed, lubrication, and other tooling and process parameters were not evaluated correctly to achieve conformity of the final product.

The experimental methods used to determine the behavior of a single material type—regarding conformity—produce satisfactory results. However, the time required to perform the necessary experiments is high. Numerical simulations may help to obtain faster results with similar reliability of experimental methods. This study intends to contribute in the choice of methods and preferential forming directions of metallic materials aiming at optimizing those forming processes. This work proposes a methodology which optimizes the stamping speed using a technique based on an interest interval comprising two initial speeds. For this purpose, it is necessary to use a computational model to simulate the forming processes able to evaluate fracture criteria for AHSS steels.

Regarding application of the continuum damage mechanics theory to forming processes, Lemaitre [9] presents a coupled model of isotropic plastic damage based on a continuous damage variable, which, in turn, is based on the "effective stress" concept. Damage is a nonlinear function of the equivalent plastic strain and is also greatly affected by the stress triaxiality. The continuum damage mechanics theory is based on the irreversible thermodynamic processes. The increase in mechanical degradation of the material is associated to the dissipated energy and can be represented by the damage variable, which is considered a state function in the thermodynamic equations. The damage identification for various metals is carried out through measurement of changes in the elasticity modulus induced by the micro-failures.

The model presented by Elgueta and Cortés [10] uses a methodology that simulates the evolution of the mechanical damage through the finite-element method. The authors present a numerical example that shows deformed regions more susceptible to micro-crack growth and, consequently, to failure when subjected to predominantly tractive stresses. Initially, regions with higher damage are located near the center line of the contact with the matrix. As metal forming increases, regions of larger damage move inside of the formed material. The presented methodology simulates damage evolution in processes involving elastoplastic deformation. In this approach, damage evolution is the mechanism that precedes failure. In other words, the damage increment—as defined in the model—is responsible for the onset of macroscopic failure.

Validation of some numerical models used in the simulation of stamping processes by finite elements was performed by comparing with experimental results, such as the works by Li et al. [11] and Wang et al. [12]. Although those authors focus their analyses mainly on numerical models for simulating stamping processes, important conclusions can be reached regarding the analysis and prediction of material fracture. Another relevant aspect is the use of advanced high strength steels in the aforementioned studies.

Wang et al. [12] developed a study for determining a critical limit of blank diameter (Limiting Drawing Ratio-LDR) for stamping. The DP600, DP800, and DP1000 are some of the steels analyzed by the authors. A comparative assessment of the test samples was performed and a failure classification was established and named "necking crack" and "shear crack." According to the authors, the critical diameter limit for the stamping blanks corresponds to a material formability indicator from which the maximum sample diameter that can be safely stamped onto a flangeless cup. In this case, a latitudinal striction was perceived for DP600 steel, whereas for DP800 and DP1000 steels, latitudinal and longitudinal strictions were detected. Thus, the authors classify the failure mode of the tested DP steels as shear with a limited localized necking.

Therefore, the analysis of the shear failure mode in stamping operations becomes essential to evaluate real formability conditions of high strength steels, as reported by Li et al. [11]. In the study conducted by those authors, the localized necking corresponds to the failure mode predominant in the steel sheets used in the industry. With the advent of the advanced high strength steels (AHSS), with smaller ductility, the fracture mode of the material was characterized by shearing, which, according to Li et al. [11], is not predicted by the forming limiting curve (FLC). The authors conclude that the forming limiting curve does not in fact allow the solution in regions where shearing fracture occurs, as a result of the folding produced during drawing, and this is an important forming characteristic of the advanced high strength steels. It is noticeable that the authors developed a study aiming at a better understanding of the origin of the shearing fracture and at predicting its occurrence with a higher precision in advanced high strength steels.

A comparative study of some existing failure criteria for metallic materials was reported by Venugopal et al. [13]. In this work, ten failure criteria were modeled for five different materials. The simulations, based on equations corresponding to each criterion, were compared to experimental results. The simulation was performed by finite elements and presents modeling details such as mesh refinement, chemical composition of materials, mechanical properties, and variables used in the failure criterion equations. The authors indicate that none of the criteria presented good results in all simulations. However, depending on the specimen geometry and material, some criteria present good results when comparing to experimental data by presenting differences smaller than 2%. Finally, Venugopal et al. [13] conclude that the failure criterion based on the maximum principal stress provides the best damage prediction when compared to theories based on the distortion energy.

According to Moreira et al. [14], the maximum plastic strain before localized necking is very important in sheet forming. The FLC is defined in the axes of the maximum and minimum principal strains obtained on the sheet plane. The curve established through linear strain trajectories remains constant during the deformation process.

When determining the FLC, it is common to simulate stress states from biaxial forming to uniaxial tensile stress condition through adequately prepared specimens. Networks of tangential or intertwined circles or squares are printed on the specimens with strictly determined dimensions. The Nakazima stamping test, described in Nakazima et al. [15], uses rectangular sheets with varying widths. Meshes or circular grids are printed on the specimens and, after forming, the deformed grids are measured to verify the stampability of the material.

The methodology of the present work aims to computationally investigate the failure mechanisms of DP600 steel. For that purpose, a computational model was developed to simulate and evaluate the forming parameters at material failure. The model was implemented through a computational code using the software ABAQUS® and obtained through a post-processing of the results.

2 Methodology

The experimental data obtained by Chemim Filho et al. [16] and Tigrinho et al. [17] were used in conjunction with the present computational model. The authors approached fracture of the DP 600 steel through variation of the blank-holder load for different forming stress and strain states. Figure 1 shows the FLC curve of the DP 600 steel determined by the Nakazima test [15].

Failure is assessed by the relation between the major and minor strains, ε_1 and ε_2, shown in Fig. 1 for the DP 600 steel obtained experimentally by Tigrinho et al. [17]. The tooling configuration was also used in simulations. The numerical

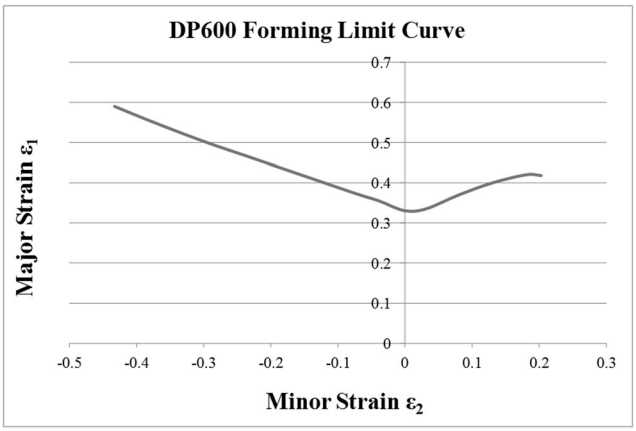

Fig. 1 DP 600 steel forming limit curve obtained by using the Nakazima stamping test [17]

simulation of the sheet forming operation makes possible to evaluate the evolution of the minor and major strains at different stages of the deformation process. Failure is assumed when the strain path in the ε_1–ε_2 space reaches the FLC shown in Fig. 1. It is relevant to mention that the von Mises material associated with an elastoplastic formulation was adopted to model the deforming sheet. Rigid die and die-sheet contact without lubrication were also used in the simulations. A finite element mesh using quadrilateral elements with standard integration were used in the ABAQUS® program.

The punch stroke used in the simulations was set to 40 mm. Initially, the stamping speed used was 4 mm/s for a DP 600 sheet measuring 200 × 200 mm and 1.5 mm thick. The unsatisfactory values of such conditions caused a catastrophic break of the specimen (Fig. 2a) and, by considering that the stop criterion is the amplitude of the punch displacement, the need for optimizing the stamping speed becomes clear. Therefore, the aim is to use an optimization method to find the ideal speed for this forming process. The optimum speed would lead to a successful forming operation (no material failure) using the minimum stamping time.

The strategy to determine the ideal forming speed is based on the bisection optimization method. This strategy reduces the search interval iteratively according to the following stages:

1. Define the initial search interval by selecting two punch speeds which prompt *rupture* "R" (high speed–upper limit) and *no rupture* "NR" (low speed–lower limit).
2. Compute the mean punch speed from values set in stage 1.
3. Simulate the forming operation for the mean punch speed, followed by assessment of the specimen (*rupture*/*no rupture*).
4. If the previous simulation prompts *rupture*, set the new speed "R" as the upper limit of the search interval. Otherwise, if the new speed results in *no rupture*, set the new speed "NR" as the lower limit of the search interval.

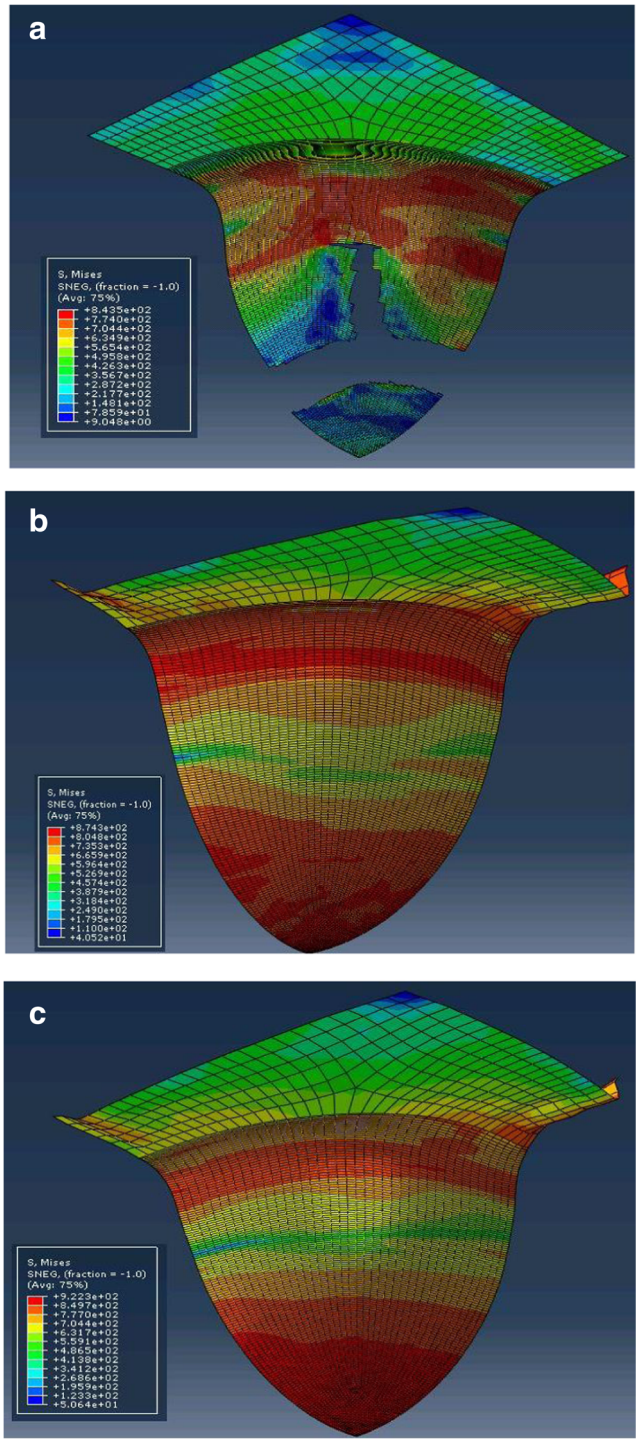

Fig. 2 Simulation results for a **a** 4 mm/s, **b** 1 mm/s, and **c** 1.1758 mm/s punch speed

5. Compute the mean punch speed of the new search interval.
6. Simulate the forming operation for the speed calculated in stage 5, followed by assessment of the specimen (*rupture*/*no rupture*).
7. Return to stage 4 and repeat the procedure until the convergence index is smaller than 1.0%.

The second punch speed selected to establish the search interval was 1 mm/s (stage 1). This punch speed is low, in industrial terms, for sheet forming. This speed was adopted based on the experimental study by Tigrinho et al. [17]. The same 40 mm of punch stroke was used in all simulations. Figure 2b shows the simulation result for such condition. It is important to point out that, for a forming speed of 1 mm/s, there is no indication of rupture by the simulation. Using the optimization method described above, after eight iterations the value of 1.1758 mm/s was obtained as an optimal result for the forming speed (Fig. 2c).

Table 1 presents the evolution of the optimization process to obtain the ideal forming speed. Noticeably, the initial search interval comprises punch speeds 1 and 4 mm/s (initial interval: stage 1), whilst the first intermediate speed is 2.5 mm/s (stage 2). The next iterative steps evaluates whether failure takes place or not in order to select the new search interval. In Table 1, "R" and "NR" mean *rupture* and *no rupture*, respectively. Convergence is evaluated by the relative difference between the previous and current punch speed, $d = |u^{(k+1)} - u^{(k)}|/u^{(k+1)} \times 100$ [%], in which u is the punch speed, k is the iteration step, and $u^{(0)} = 1.0$ mm/s (lower limit of the initial interval). Convergence is assumed when the relative difference is $d \leq 1.0\%$ (stage 7).

Therefore, this study shows that, when compared to experimental adjustments of the process, after a few iterative steps requiring small computational time, it is possible to determine the ideal stamping speed. In order to accomplish the task, the software requires the material parameters and geometrical data, such as die, punch, and sheet dimensions.

The strategy proposed in the present study has great potential to save time in the process preparation and helps to achieve better productivity levels compliant with the quality requirements through the conformity of the final product.

Table 1 Evolution of the iterative process: punch speed [mm/s] × rupture/non-rupture

Simulation step	Punch speed [mm/s]	Rupture/non-rupture	Convergence index d [%]
Initial search interval	4.0 (upper limit) 1.0 (lower limit)	R NR	–
#1	2.5000	R	60.000
#2	1.7500	R	42.857
#3	1.3750	R	27.273
#4	1.1875	R	15.789
#5	1.0938	NR	8.571
#6	1.1406	NR	4.110
#7	1.1641	NR	2.013
#8	1.1758	NR	0.997

Table 2 Chemical composition of DP 600 steel

Chemical composition of DP600 steel (mass parts in %)												
Laboratory test, this work												
C	Si	Mn	P	S	Al	Cr	Nb	Zr	Ti	Ni	Mo	Cu
0.086	0.053	1.739	0.027	0.007	0.031	0.048	0.028	0.006	0.004	0.029	0.226	0.0094
Provided by the manufacturer												
C	Si	Mn	P	S	Al	Cr	Nb	V	Ti	Ni	Mo	N
0.07	0.01	1.66	0.019	0.005	0.043	0.03	0.015	< 0.005	< 0.005	0.02	0.16	0.0058
Kim et al. [18]												
C	Si	Mn	P	S	Al	Cr	Nb	V	Ti	Ni	Mo	Cu
0.092	0.123	1.7	0.016	0.001								
Uthaisangsuk et al. [19]												
C	Si	Mn	P	S	Al	Cr	Nb	V	Ti	Ni	Mo	Cu
0.072	0.246	1.58	0.015	0.001	0.031	0.053						0.010
Farabi et al. [20]												
C	Si	Mn	P	S	Al	Cr	Nb	V	Ti	Ni	Mo	Cu
0.09	0.36	1.84		0.005	0.05	0.02					0.01	0.03

3 Material characterization

In order to ascertain a proper classification of the steel adopted in the present study, a chemical analysis of the material, metallography, and tensile tests was performed. As reference, the corresponding data provided by the manufacturer and also by other works are also presented. The main characterization results of the material used in the simulation are presented in Tables 2 and 3.

The tension tests performed with specimens removed at 0°, 45°, and 90° in relation to the sheet rolling direction provide information regarding the mechanical properties of the material, such as the yield strength (YS), ultimate strength (US), and elongation (e). These properties characterize the material in relation to its maximum strength limit, (US), maximum stresses attained at the end of elastic deformation and plastic strain onset, (YS), and maximum elongation (e) of the material up to catastrophic fracture.

Table 3 Comparison of mechanical properties of DP 600 steel

Mechanical properties of DP600 steel			
Properties	YS (MPa)	US (MPa)	e (%)
Tensile tests, this work	410	640	28.5
Provided by the manufacturer	385	621	23.9
DP600; Huh et al. [21]	422	632	26.9
DP590; Kim et al. [18]	380	619	28.2
DP600; Wang et al. [12]	412	676	27.0

4 Numerical simulation

This section discusses evolution of the strains at selected locations with the objective of a better understanding of the failure process. The strains analyzed in the present study are calculated by the differences between the size of the elements (before and after forming) of the simulated mesh at 0°, 45°, and 90° in relation to the sheet rolling direction and along the sheet thickness.

The region selected for the analysis is parallel to the main crack (Fig. 3) in order to follow the crack evolution in its direction of propagation. Noticeably, the selected elements are those adjacent to the main crack, but not part of it, i.e., immediately next to the rupture site. The analyzed points consist of 20 elements of the simulated mesh, for which an absolute measure of the logarithmic strain (OL) is computed in all four directions described in the previous paragraph.

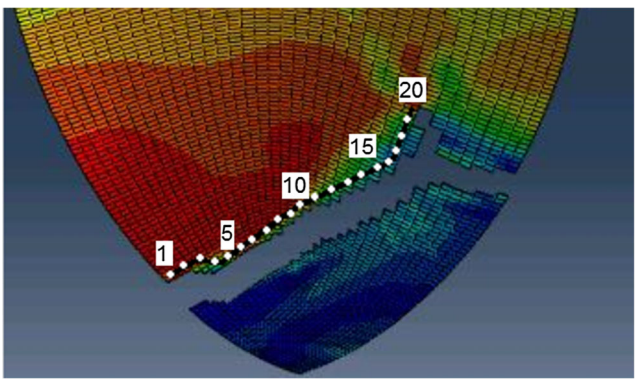

Fig. 3 Analyzed area focusing on the strain parallel to the crack

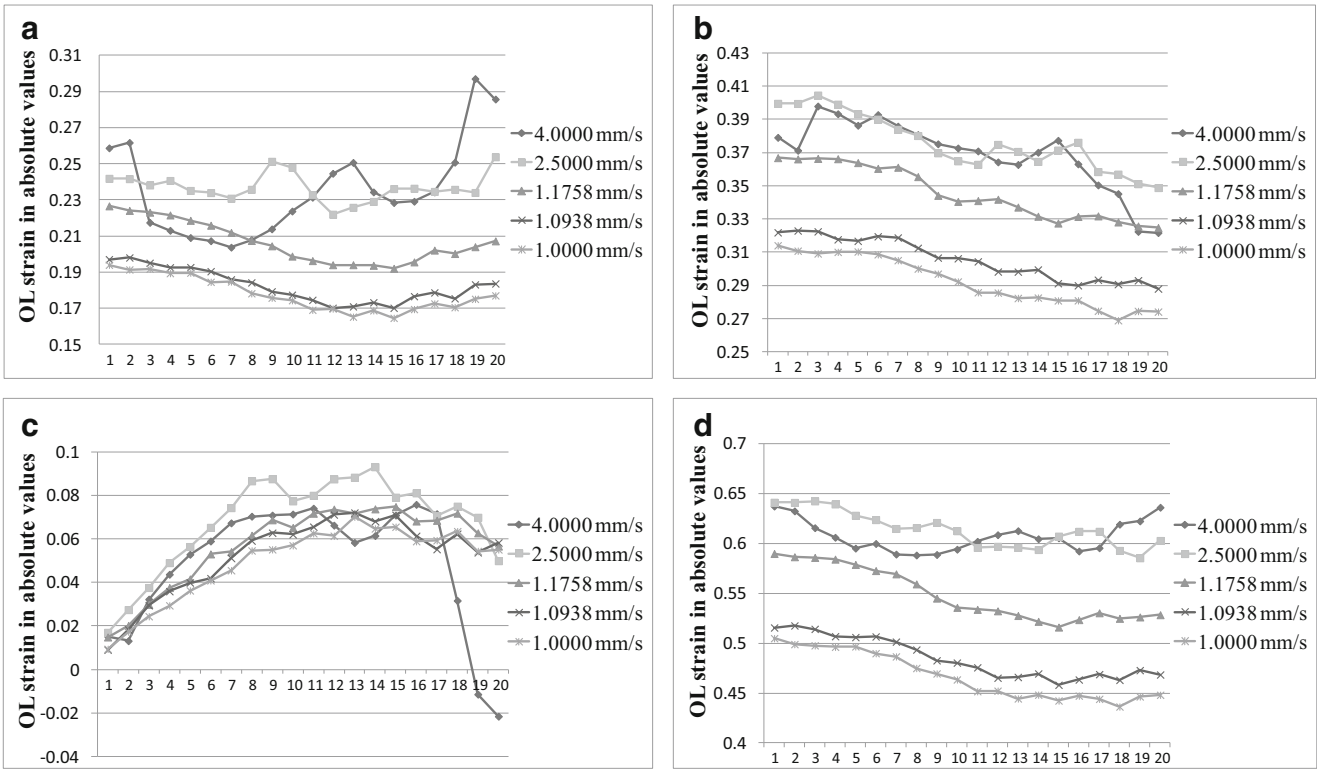

Fig. 4 Strain parallel to the main crack **a** in the sheet rolling direction, **b** at 90° in relation to sheet rolling direction, **c** at 45° in relation to sheet rolling direction, and **d** in sheet thickness

It is also relevant to mention that, in cases which the punch speed is smaller than the critical value required for material failure, the analyzed elements were chosen by calculating the medium points of locations at which rupture took place in previous analyses. The elements are identified by numbers which represent their corresponding positions in the simulated mesh. Thus, the point is located very close to the possible rupture site, if elongated to the amplitude in the simulation.

The strains of the elements next to the crack (Fig. 3) are shown in Fig. 4a–d. In those figures, evolution of the logarithmic strains are presented for each component, i.e., (Fig. 4a) in the rolling direction, (Fig. 4b) perpendicular to rolling, (Fig. 4c) at 45° in relation to the rolling direction, and (Fig. 4d) along the sheet thickness.

Table 4 Parameters of the experimental procedure

Parameter	Value/characteristics
Material	DP 600 steel
Blank	200 × 200 mm
Thickness	1.5 mm
Mesh size	4 mm
Punch diameter	65 mm
Blank-holder diameter	165 mm
Blank-holder pressure	50 bar
Lubrication	No

The cases portrayed in Fig. 4a–d include the maximum (4.0 and 2.5 mm/s), minimum (1.0 and 1.0938 mm/s), and optimal (1.1758 mm/s) punch speeds. It can be observed in Fig. 4a–d that higher speeds lead to larger strains or strains with larger variations in all directions (0°, 90°, and 45°) and along the sheet thickness. The optimal speed (1.1758 mm/s) is characterized by intermediate values of the strain components with more uniform and smoother behavior than those which prompted material failure. Therefore, the results show that, as the punch speed increases, strains also increase, eventually causing failure onset (criterion given by the FLC presented in Fig. 1), which in turn leads to larger variations in all directions.

4.1 Results and discussions

Experimental procedures aiming at validating the simulation results, mainly the variation of the stamping depth

Table 5 Results of the experimental procedure

Sample	Speed [mm/s]	Depth [mm]
1	4.0000	24.8
2	2.5000	25.2
3	1.1758	26.1
4	1.0000	25.6

with respect to the forming speed, were performed. The forming depth was constant for all simulations, in order to comply with the stop and evaluation criterion of the final results of the conformed sheets in the case study at issue. That is, having the forming parameters adjusted to the same values of the simulation, the comparison of the results presented the same referential for the evaluation of uniformity (or the lack of), in the strain evolution due to the variation of speed.

Table 4 presents the blank and tooling characteristics, as well as the forming parameters used in the experimental procedure.

The results of the experimental procedure, performed for four speeds, can be verified in Table 5. Those speeds were chosen because they reproduce the simulation with variation between extremes, i.e., the highest speeds (4.0 and 2.5 mm/s) in comparison against the lowest speed (1.0 mm/s) and the optimal speed suggested by the present methodology (1.1758 mm/s). The choice of those speeds was based on the simulated values within the upper and lower limits.

5 Conclusions and final remarks

The present methodology proved to be effective by presenting a faster and reliable solution (regarding actual experiments) for the optimization of forming procedures of metallic sheets with respect to material failure. Optimization of the forming time by determining the ideal forming speed was presented. The proposed technique finds the maximum possible stamping speed without failure onset. The methodology prompted a high convergence rate, approximating the optimum punch speed with few iterations. The optimization method requires material data, as well as the characteristics of the process and tooling. The methodology has a great potential to gain in productivity with greater reliability in the final result of the final product, i.e., it is able to save time in the process preparation and helps to achieve better productivity levels. The simulations show that lower forming speeds make possible to achieve greater forming depths, whereas higher stamping speeds may cause abrupt and premature rupture. Furthermore, the results show that strains in all analyzed elements are more uniformly distributed when forming takes place at lower strain rates. Finally, the numerical results presented good approximation to those obtained by experiments, for which larger forming depth were associated with lower speeds, even with a procedure that presented a small amplitude, regarding depth, when compared to the deep drawing performed in the industry worldwide.

Acknowledgements The authors thank the Usiminas and Arcelor Mittal for supplying the steels used in the study.

Funding information The study receives financial support from the CNPq (National Council for Scientific and Technological Development).

References

1. Andrade SL, TAISS JM, Rosa LK (2002) O aço no automóvel do futuro. In: 57 Congresso da Associação Brasileira de Metalurgia e Materiais, 2002. Anais, São Paulo
2. De Cooman BC (2004) Structure-properties relationship in TRIP steels containing carbide-free bainite. Curr Opin Solid State Mater Sci 8:285–303
3. Grajcar A, Adamczyk J (2005) Structure and mechanical properties of DP-type and TRIP-type sheets obtained after the thermomechanical processing. J Mater Process Technol 162-163:267–274
4. Rashid MS (1977) GM 980X – Potential Applications and Review. *International* Automotive Engineering Congress and Exposition. S.A.E. Technical Publication no 770211. Detroit, 12 p., February–March 1977
5. Sampaio AP, Martins CA, Souza PC (1998) Caracterização da Conformabilidade de Aço Livre de Intersticiais – IF – Produzido Via Recozimento em Caixa na Companhia Siderúrgica Nacional. In: CONFERÊNCIA NACIONAL DE CONFORMAÇÃO DE CHAPAS, 1., 1998. UFRGS – Centro de Tecnologia, Porto Alegre, pp 89–100
6. Keeler SP (1965) Determination of forming limits in automotive stampings. Sheet Met Ind 42:683–691
7. Goodwin GM (1968) Application of strain analyses to sheet metal forming problems in the press shop. Metall Italiana 60:764–774
8. Woodthorpe J, Pearce R (1969) The effect of r and n upon the forming limit diagrams of sheet metal. Sheet Metal Industries: 1061–1067
9. Lemaitre J (1985) A continuous damage mechanics model for ductile fracture. J Eng Mater Technol 107:83–89
10. Elgueta M, Cortés C (1999) Application of continuum damage theory in metalforming processes. J Mater Process Technol 95:122–127
11. Li Y, Luo M, Gerlach J, Wierzbicki T (2010) Prediction of shear-induced fracture in sheet metal forming. J Mater Process Technol 210:1858–1869
12. Wang WR, He CW, Zhao ZH, Wei XC (2011) The limit drawing ratio and formability prediction of advanced high strength dual-phase steels. Mater Des 32:3320–3327
13. Venugopal Rao A, Ramakrishnan N, Krishna Kumar R (2003) A comparative evaluation of the theoretical failure criteria for workability in cold forging. J Mater Process Technol 142:29–42
14. Moreira LP, Sampaio AP, Ferron G, Lacerda AC (2003) Análise numérica e experimentação da influência da espessura inicial das deformações limites em chapas. In: CONFERÊNCIA NACIONAL DE CONFORMAÇÃO DE CHAPAS, 6., 2003, Porto Alegre. Anais... Porto Alegre: UFRGS – Centro de Tecnologia, pp 39–49
15. Nakazima K, Kikuma T, Hasuka K (1968) Study on the formability of steel sheets. Yawata Technical Report:111–141
16. Chemin Filho RA, Tigrinho LMV, Barreto Neto RC, Marcondes PVP (2013) An experimental approach for blankholder force determination for DP600 with different material flow strain rates in the flange during stamping. J Eng Manuf 227(3):417–422
17. Tigrinho LMV, Chemin Filho RA, Marcondes PVP (2013) Fracture analysis approach of DP600 steel when subjected to different stress/

strain states during deformation. Int J Adv Manuf Technol 69: 1017–1024

18. Kim SB, Huh H, Bok HH, Moon MB (2011) Forming limit diagram of auto-body steel sheets high-speed sheet metal forming. J Mater Process Technol 211:851–862
19. Uthaisangsuk V, Prahl U, Bleck W (2011) Modelling of damage and failure in multiphase high strength DP and TRIP steels. Eng Fract Mech 78:469–486
20. Farabi N, Chen DL, Li J, Zhou Y, Dong SJ (2010) Microstructure and mechanical properties of laser welded DP600 steel joints. Mater Sci Eng A 527:1215–1222
21. Huh H, Kim SB, Song JH, Lim JH (2008) Dynamic tensile characteristics of TRIP-type and DP-type steel sheets for an auto-body. Int J Mech Sci 50:918–931